

This state is clearly an eigenstate of the total number of electrons, and so is that of Eq. (2) with Eq. (7). When  $\gamma=0$ , this state is equivalent to that of Yosida by replacing the electron operator by the hole operator.

<sup>6</sup>Using our wave function,  $\lambda_0 = \mu \exp[-4/3N_0|J|]$ , where  $\mu$  is the usual cutoff energy (of order of the Fermi energy). This same expression was obtained by Heeger and Jensen (Ref. 2).

<sup>7</sup>We define the susceptibility as  $\chi(H) = (\partial/\partial H)\{\mu_B(n_{d\uparrow} - n_{d\downarrow})\}$  for all fields. At low field, a similar result is obtained by Takano and Ogawa [Progr. Theoret. Phys. **35**, 343 (1966)] by the usual Green's function method. However, their result is different from ours by the factor  $\pi^{-1}$ .

<sup>8</sup>This critical field corresponding to the critical temperature of 10°K is twice that of Ref. 3. The reason for this discrepancy between the two experiments is unclear.

## EVIDENCE FOR A TRIPLET STATE OF THE SELF-TRAPPED EXCITON IN ALKALI-HALIDE CRYSTALS

M. N. Kabler and D. A. Patterson

U. S. Naval Research Laboratory, Washington, D. C.

(Received 7 August 1967)

The lifetimes and polarizations of intrinsic recombination radiation from alkali-halide crystals at low temperature are interpreted in terms of two self-trapped exciton states, one predominantly singlet, the other triplet in character. This is the first strong evidence for the triplet assignment. The variation with crystal of the triplet-state lifetime is attributed to effects of the different halogen spin-orbit couplings and the varying degrees of axial relaxation in the self-trapped configuration.

Under high-energy excitation at low temperature, pure alkali-halide crystals luminesce with high efficiency. This luminescence has been shown to arise primarily from intrinsic radiative recombination of electrons and self-trapped holes ( $V_k$  centers).<sup>1-3</sup> The emission spectra are closely related to those resulting from excitation with light in the exciton absorption bands.<sup>4</sup> The term "self-trapped exciton" appropriately describes the luminescent center, which may be regarded simply as a halide-ion pair in a bonding excited state. The  $\langle 110 \rangle$  bond axis is evident from the polarization of the luminescence.<sup>5</sup>

Table I shows data obtained in this laboratory and elsewhere<sup>2,3,6</sup> on peak energies, polarizations, and lifetimes for self-trapped exciton emission bands at liquid-helium temperature (LHeT). Although extensive data exist on intrinsic luminescence excited by ultraviolet light,<sup>4,7</sup> we have for consistency included in Table I only data obtained with x-ray and high-energy-electron excitation. Both  $\sigma$  and  $\pi$  transitions occur in general, the former with short (allowed) lifetimes  $\tau_{lm}$ , the latter, at lower energy, with longer (apparently forbidden) lifetimes  $\tau_{km}$ . This lifetime correlation was evident in previous experiments on KI.<sup>8</sup> The  $\sigma$  transition has not been observed in four of the crystals. Only RbI exhibits a third, possibly intrinsic, band of any consequence, and

it is relatively weak at LHeT.<sup>3</sup> The half-widths of the bands in Table I range from 0.3 to 0.7 eV.

The experimental methods have been described,<sup>1</sup> except for the lifetime measurements; these employed standard electronic techniques to detect luminescent decay after excitation by a 15-MeV electron pulse ( $\approx 20$  nsec duration) from the Naval Research Laboratory Linac. The accuracy of  $\tau_{lm}$  was limited by instrumental resolution. Since the radiative efficiencies are high at LHeT, the lifetimes will be identified with the reciprocals of radiative-transition probabilities.

We shall discuss states of the self-trapped exciton in terms of those of a diatomic rare-gas molecule. This analogy is appropriate because of the close similarities between the electronic configurations of a free rare-gas atom and a free (unrelaxed) exciton,<sup>9</sup> and because of the close experimental relationship of the self-trapped exciton to the  $V_k$  center (diatomic molecular ion).<sup>1</sup> The ground state is then  $(\sigma_g np)^2 (\pi_u np)^4 (\pi_g np)^4 (\sigma_u np)^2 {}^1\Sigma_g^+$ , which is unstable; the lowest self-trapped exciton states are  $\dots (\sigma_u np) [\sigma_g (n+1)s]^3 {}^1\Sigma_u^+$ , which are bound.<sup>10</sup> It is evident that the  $\tau_{lm}$  and the polarization of the  $\sigma$  transition are consistent with  ${}^1\Sigma_u^+ \rightarrow {}^1\Sigma_g^+$ . For the  $\pi$  transition, the variation of  $\tau_{km}$  with anion appears consistent with  ${}^3\Sigma_u^+ \rightarrow {}^1\Sigma_g^+$ , for which multiplicity forbiddenness is broken by mixing due to the halo-

Table I. Emission-band peak energies and lifetimes for self-trapped exciton transitions. Parameters relevant to the analysis of the  $\pi$  transition are also shown; they are defined in the text. All energies are in units of eV.

	$\sigma$ Transition		$\pi$ Transition						
	$E_{1m}$	$\tau_{1m}$ ( $10^{-9}$ s)	$E_{km}$	$\tau_{km}$ ( $10^{-6}$ s)	$E_1^d$	$\zeta^e$	$E_c$	$b^2$	$ \langle s   \underline{r}   m \rangle ^2$ ( $10^{-18}$ cm $^2$ )
NaCl	5.6 <sup>a</sup>	$\lesssim 5$	3.38 <sup>a</sup>	295	7.96	0.073	1.3	0.00049	3.8
KCl	-	-	2.32	5000	7.76	0.073	0.8	0.00025	1.1
RbCl	-	-	2.27	5500	7.51	0.073	0.7	0.00026	1.1
NaBr	-	-	4.60	0.49	6.68	0.306	1.3	0.106	2.9
KBr	4.42	$\approx 9$	2.27	130	6.77	0.306	0.8	0.0069	1.6
RbBr	4.20	$\approx 11$	2.10	180	6.60	0.306	0.7	0.0065	1.6
NaI	-	-	4.20 <sup>b, c</sup>	0.09 <sup>b</sup>	5.56	0.629	1.3	0.48	4.1
KI	4.15 <sup>c</sup>	$\approx 9$	3.34	4.4	5.80	0.629	0.8	0.100	0.9
RbI	3.95 <sup>c</sup>	$\approx 9$	2.30 <sup>c</sup>	11	5.70	0.629	0.7	0.053	2.2

<sup>a</sup>Polarization not yet measured.

<sup>b</sup>Data of Ref. 6.

<sup>c</sup>Polarization from Refs. 2 and 3.

<sup>d</sup>Data of J. E. Eby, K. J. Teegarden, and D. B. Dutton, Phys. Rev. **116**, 1099 (1959).

<sup>e</sup>See, e. g., R. S. Knox and N. Inchauspé, Phys. Rev. **116**, 1093 (1959).

gen spin-orbit (s-o) coupling of  ${}^1\Pi_u$  character into the  ${}^3\Sigma_u^+$  state. The validity of this mechanism is our present concern, particularly with regard to the observed strong dependence of  $\tau_{km}$  on the cation as well as the anion.

The  ${}^1\Pi_u$  electronic configuration which mixes most strongly with  ${}^3\Sigma_u^+$  and thus makes the largest contribution to the  $\pi$  transition will in all likelihood be  $(\sigma_g n p)^2 (\pi_u n p)^3 (\pi_g n p)^4 (\sigma_g n p)^2 \times [\sigma_g (n+1) s]$ . States involving the higher  $\pi$  orbitals can hardly contribute significantly.<sup>11</sup> These  ${}^3\Sigma_u^+$  and  ${}^1\Pi_u$  states, along with the two states having the hole in the  $\sigma_g n p$  and  $\pi_g n p$  orbitals, are represented in Fig. 1 by the dashed potential curves, which are schematic and which omit exchange and s-o coupling. Figure 1 is a composite configuration-coordinate diagram in which  $r_a$  and  $r_c$  represent changes in the halide-ion separation and the cubic relaxation, respectively. In the limit of small electron-hole interaction, the dashed curves

will be just  $V_k$ -center potential curves.<sup>12</sup> The  ${}^1\Sigma_g^+$  ground state and the  ${}^3\Sigma_u^+$  and  ${}^1\Pi_u$  exciton states with exchange and s-o coupling included are represented schematically by solid curves in Fig. 1. As shown, the two self-trapped exciton states originate from the states associated with the s-o doublet in absorption; in the  $jj$ -coupling limit, these latter states correspond to hole  $j$  values of  $\frac{3}{2}$  or  $\frac{1}{2}$ .<sup>13</sup>

Let us now estimate the admixture of  ${}^1\Pi_u$  into  ${}^3\Sigma_u^+$ . Under the s-o coupling  $H_{SO}$ , the actual wave functions  $|k\rangle$  become the linear combinations  $a|t\rangle + b|s\rangle$  and  $a|s\rangle - b|t\rangle$ , where  $|t\rangle$  and  $|s\rangle$  represent uncoupled  ${}^3\Sigma_u^+$  and  ${}^1\Pi_u$  functions, respectively.  $H_{SO}$  can be diagonalized to give  $a^2$  and  $b^2$  in terms of the matrix element  $\langle s | H_{SO} | t \rangle = \frac{1}{2}\zeta$  and the energy separation  $E_{st}$  of  $|s\rangle$  and  $|t\rangle$  at the equilibrium  $r_a$ .<sup>14</sup>  $\zeta$  is the s-o coupling parameter for the halide-ion  $p^5s$  configuration; as is customary, the measured  $\zeta$  values for the  $p^5$  configuration of

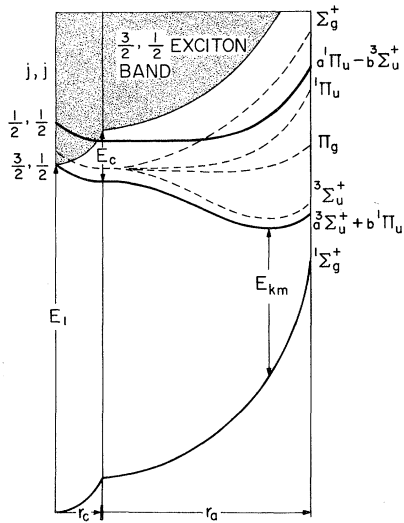


FIG. 1. Schematic potential curves for self-trapped excitons. The configuration coordinates  $r_c$  and  $r_a$  measure departures from the perfect lattice configuration due to cubic and axial relaxations, respectively. Of the many possible states, only those relevant to the discussion of the  $\pi$  transition are shown. The dashed curves do not include exchange or spin-orbit coupling.

the free halogen atom will be used (Table I).<sup>13</sup>

Both  $E_{st}$  and a portion  $E_l - E_c - E_{km}$  of the Stokes shift increase monotonically with axial relaxation  $r_a$ . As noted in Fig. 1,  $E_l$  is the energy of the first exciton absorption band,  $E_{km}$  is the emission energy, and  $E_c$  is that part of the Stokes shift due to  $r_c$ . A crude though adequate estimate of  $E_{st}$  may thus be obtained by simply setting  $E_{st} = \frac{1}{2}(E_l - E_c - E_{km})$ . The factor  $\frac{1}{2}$  is chosen to make  $E_{st}$  roughly consistent with  $V_k$ -center absorption energies<sup>15</sup> for crystals in which the triplet exciton gives the largest Stokes shift and consequently has an equilibrium  $r_a$  nearest that of the  $V_k$  center. For KCl we take  $E_c$  to be Wood's calculated exciton Stokes shift (cubic only)<sup>16</sup>; lacking a better procedure, values for the other crystals have been scaled from this one roughly in proportion to  $F$ -center Stokes shifts.<sup>17</sup>  $E_l$ ,  $E_c$ ,  $\zeta$ , and the resulting  $b^2$  values are included in Table I.

The spontaneous emission probability between nondegenerate states  $|k\rangle$  and  $|m\rangle$  is

$$\tau_{km}^{-1} = (4e^2 n E_{km}^3 / 3\hbar^4 c^3) (\xi_{\text{eff}} / \xi_0)^{-2} |\langle k | \vec{r} | m \rangle|^2, \quad (1)$$

where  $n$  is the refractive index at  $E_{km}$ .<sup>18</sup> The

value of the effective-field ratio is in principle  $1 < \xi_{\text{eff}} / \xi_0 \leq 2$  and should vary little with crystal; we set  $\xi_{\text{eff}} / \xi_0 = 1$  for convenience. Only the singlet part  $b|s\rangle$  of  $|k\rangle$  contributes to the matrix element, since  $|m\rangle$  represents  $^1\Sigma_g^+$ . Using the  $\tau_{km}$ ,  $E_{km}$ , and  $b^2$  from Table I,<sup>19</sup> Eq. (1) yields  $|\langle s | \vec{r} | m \rangle|^2$ . Its variation from crystal to crystal, if the model is valid, should be slight compared with that of  $\tau_{km}$ . Table I shows this to be the case. The strong dependence of  $\tau_{km}$  on the cation is seen to be accountable partly through the  $E_{km}$ <sup>3</sup> in Eq. (1) and partly through  $E_{st}$ . It is inherent in the model that the variations in  $E_{km}$  and  $E_{st}$  for a given anion are largely due to variations in the equilibrium  $r_a$ .<sup>20</sup>

For the allowed  $\sigma$  transition, Eq. (1) gives  $|\langle l | \vec{r} | m \rangle|^2 \approx 2 \times 10^{-17} \text{ cm}^2$  for each of the five crystals, where  $|l\rangle$  represents  $^1\Sigma_u^+$ . The nature of the orbitals on which our analysis has been based would lead one to expect  $|\langle l | \vec{r} | m \rangle| \geq |\langle s | \vec{r} | m \rangle|$ , which is seen to hold true generally.

It is thus apparent that, with reasonable values for the relevant physical parameters, the relaxed-exciton model is consistent with the measured lifetimes of the  $\pi$  transition and their variation with crystal. There is presently no indication that alternative mechanisms can produce the large lifetime variations. One such mechanism would have the transition allowed but long lived because of a diffuse excited-electron orbital.<sup>16</sup>

Attempts to observe epr in the relaxed-triplet-exciton state are currently underway. A full account of the present work will be published shortly.

The authors wish to thank R. S. Knox, M. H. Reilly, C. C. Klick, W. B. Fowler, and M. J. Marrone for many helpful discussions, T. L. Gilbert for a copy of his Ghent Lecture Notes, and T. F. Godlove and members of the Linac staff for considerable technical assistance.

<sup>1</sup>M. N. Kabler, Phys. Rev. **136**, A1296 (1964).

<sup>2</sup>R. B. Murray and F. J. Keller, Phys. Rev. **137**, A942 (1965).

<sup>3</sup>R. B. Murray and F. J. Keller, Phys. Rev. **153**, 993 (1967).

<sup>4</sup>For a review, see K. Teegarden, in *Luminescence of Inorganic Solids*, edited by P. Goldberg (Academic Press, Inc., New York, 1966), Chap. 2.

<sup>5</sup>Although  $D_{2h}$  is the appropriate point group for the self-trapped excitation,  $D_{\infty h}$ , the group of a diatomic

molecule, is adequate to represent the experimental results. In  $D_{\infty h}$  the possible transitions are termed  $\sigma$  or  $\pi$  according to whether the electric vector of the radiation is parallel or perpendicular to the axis.

<sup>6</sup>W. Van Sciver and L. Bogart, IRE Trans. Nucl. Sci. 5, 90 (1958).

<sup>7</sup>J. Ramamurti and K. Teegarden, Phys. Rev. 145, 698 (1966).

<sup>8</sup>R. K. Ahrenkiel, Solid State Commun. 4, 21 (1966). These lifetimes were obtained by a somewhat different method and are a factor of 2 lower than our values.

<sup>9</sup>K. Teegarden and G. Baldini, Phys. Rev. 155, 896 (1967).

<sup>10</sup>G. Herzberg, Molecular Spectra and Molecular Structure: I. Spectra of Diatomic Molecules (D. Van Nostrand Company, Inc., Princeton, New Jersey, 1950), 2nd ed.

<sup>11</sup>The  $\dots(\sigma_u n p)(\pi_g n d)^1\Pi_u$  and  $\dots(\sigma_u n p)[\pi_g(n+1)p]^1\Pi_u$  configurations contribute to  $\tau_{km}$  only to the extent that  $\sigma_g n d$  and  $\sigma_g(n+1)p$  orbitals contribute to  $^3\Sigma_u^+$ , because only  $p-p$  and  $d-d$  (not  $s-p$ ) atomic mixtures occur in first order. Furthermore, the  $nd$  and  $(n+1)p$   $s-o$  couplings would be appreciably smaller than the  $np$ . Note that  $s-o$  coupling mixes only states which (1) have the same axial component of total angular momentum, (2) have the same parity, and (3) differ in the orbital of only one electron. Mixing of  $^3\Pi_g$  into the ground state

is also unimportant.

<sup>12</sup>The dashed potential curves of Fig. 1 are closely related to those for hole self-trapping given by T. L. Gilbert, Notes for North Atlantic Treaty Organization Summer School in Solid State Physics, Ghent, Belgium, 1966 (unpublished). See also T. P. Das, A. N. Jette, and R. S. Knox, Phys. Rev. 134, A1079 (1964).

<sup>13</sup>R. S. Knox and N. Inchauspé, Phys. Rev. 116, 1093 (1959).

<sup>14</sup>For procedures related to the evaluation of  $\langle s | H_{SO} | t \rangle$ , see L. Goodman and V. G. Krishna, Rev. Mod. Phys. 35, 541 (1963). The hole orbitals are taken to be linear combinations of  $p$  atomic orbitals only, any  $s$  admixture being neglected.

<sup>15</sup>C. J. Delbecq, W. Hayes, and P. H. Yuster, Phys. Rev. 121, 1043 (1961).

<sup>16</sup>R. F. Wood, Phys. Rev. 151, 629 (1966).

<sup>17</sup>P. Podini and G. Spinolo, Solid State Commun. 4, 263 (1966). The  $F$ -center Stokes shift is known to be primarily due to cubic relaxation.

<sup>18</sup>W. B. Fowler and D. L. Dexter, Phys. Rev. 128, 2154 (1962).

<sup>19</sup>Where necessary,  $n$  has been estimated (only two-figure accuracy is required) by extrapolating extant data to the relevant wavelengths and to LHeT.

<sup>20</sup>This matter will be discussed further, M. N. Kabler and M. H. Reilly, to be published.

## FIELD-INDUCED CHANGES IN THE BAND STRUCTURE AND FERMI SURFACE OF NICKEL\*

L. Hodges,<sup>†</sup> D. R. Stone, and A. V. Gold<sup>‡</sup>

Institute for Atomic Research and Department of Physics, Iowa State University, Ames, Iowa

(Received 30 June 1967)

The de Haas-van Alphen effect has been studied in spherically shaped crystals of nickel. The unusual angular variations in the frequencies arising from the  $X_5$  hole pockets can be accounted for in terms of an interpolation scheme which includes the effect of spin-orbit coupling. The sizes of the hole pockets depend markedly on the axis of spin quantization, i.e., on the direction of the applied magnetic field.

A self-consistent calculation of the ferromagnetic band structure of nickel was recently carried out<sup>1</sup> incorporating correlation effects through the use of an intra-atomic Coulomb interaction. This calculation was based on a simple interpolation scheme for paramagnetic transition metals and made use of several parameters obtained from first-principles augmented-plane-wave band calculations; use was also made of the experimentally determined magneton number as well as other experimental information such as the size of the [111] "neck" in the copperlike sheet of the Fermi surface as determined by the low-frequency de Haas-van Alphen oscillations of Joseph and Thorsen.<sup>2</sup> The limited nature of this experimental information coupled with the uncertain-

ties inherent in the first-principles band structure prevented an exact determination of the position of some of the energy bands near the Fermi surface, and as a consequence the size, shape, and even the existence of a number of small hole pockets in the Fermi surface could not be accurately ascertained. In this paper we wish to present the results of further studies of the de Haas-van Alphen effect in spherical samples of nickel and to discuss the relevance of these results to the band structure. Excellent agreement with experiment is found when the original interpolation scheme<sup>1</sup> is modified by readjusting certain parameters<sup>3</sup> and by including the effects of spin-orbit coupling; this interaction leads to variations in the band structure (and in the Fermi surface) which